Journal of Education for Pure Science- University of Thi-Qar
Vol.13, No.3 (Sept.2023)
Website: jceps.utq.edu.iq Email jceps@eps.utq.edu.iq

DOI: http://doi.org/10.32792/utq.jceps.10.01.01

Prepare heterostructure of MoS2/TiO2 solar cell via simple two-steps by hydrothermal method

Sajjad Said [1], **Alaa AL-Hilo [2,*]**

sajadsaeedsajad2021@mail.com

.[1] Basrah University, College science, Physics Department

[2] Basrah University, College science, Physics Department.

Received 11/6/2023, Accepted 9/7/2023, Published 21/9/2023

Abstract:

Organic dyes employ in traditional Dye-sensitized solar cells (DSSC) results in both high cost and low stability under light exposure. In this study, we present an inorganic semiconductor heterostructure solar cell based in ordered thin film of MoS2 deposited on one-dimensional nanorods array of TiO2 which were produced via simple two-steps by hydrothermal method. The solar cell MoS2/TiO2 heterostructure exhibit a good fill factor, and a greatly enhanced power conversion efficiency. The research presented here will provide a path for creating heterostructure inorganic materials for highly efficient solar cells .

Keywords: inorganic semiconductor, TiO2, MoS2, nanorods, solar cells, hydrothermal method.

1-Introduction

In recent decades, a significant increase in research literature has focus in the solar energy conversion for generate solar cells [1,2]. Titanium Dioxide TiO_2 semiconductor nanomaterials exhibiting various morphologies are considered the most favorable candidates for photoanode in solar cells [3, 4]. Among the numerous TiO_2 nanostructures including nanotubes, nanowires, and nanorods arranged in ordered to one-dimension array, that have demonstrated great potential for use in DSSC. This is due to their potential to offer direct pathways for efficient charge transfer and also collection [5,6]. Furthermore, light harvesting is facilitated by the vertical alignment and ordered arrangement of nanostructures due to many internal reflections between neighboring construction blocks [7,8]. Also, the 1D TiO_2 nanostructures might also provide a special three-dimensional (3D) architecture that would facilitate the simple entry and diffusion of the electrolyte [8]. Many

researchers focusing on TiO_2 due to unique features which include chemical and thermal stability, low toxicity, and environmental safety, as well as its affordability[9]. The hydrothermal method is an inexpensive, safe method, and simple technique for TiO_2 growth on fluorine-doped tin oxide (FTO) coated glass- substrate without the requirement for seed layers. This due to the similar crystal structures and low lattice mismatch between FTO and TiO_2 [10]. In the fact, the TiO_2 semiconductor exhibits light absorption in the ultraviolet (UV) range due to its high band gap energy of (~ 3.2) eV which reduce the utilization of sunlight [11-13]. One of the promising approaches to address these issues is to develop inorganic sensitizers with good optical absorption and good chemical stability. Molybdenum Disulfide (MoS_2) a two-dimensional semiconductor similar to Graphene with fascinating electrical and optical features [14]. Bulk MoS_2 is composed of several S-Mo-S stacking layers that are weakly bound together by weakly Van der Waals forces, While few-layer MoS_2 showed promise in optical and electrical applications [15]. The single - layer MoS_2 exhibits an sandwich structure where two S atoms are hexagonally packed around Mo atoms in the center [16 ,17]. MoS_2 in bulk was typically utilized as a mechanical lubricant, although single- MoS_2 has a narrow band gap of (1.2-1.9) eV having the proper band structure to promotes high photo – response within the visible light spectrum [18,19].

In this study, we grew single - layer MoS_2 in the one-dimension nanorods of TiO_2 using a simple two-step hydrothermal method . MoS_2 demonstrated that is an good inorganic sensitizer, significantly enhancing the light-harvesting and charge separation capabilities of the TiO_2 photoanode.

.

2- Experimental

TiO_2 nanorods array were grown using a hydrothermal method on a Conductive FTO substrate (1cm*1.5 cm). To achieve this, the FTO substrate was placed inside a sealed Teflon-lined stainless steel autoclave along with a solution containing Titanium butoxide (0.5 ml), Deionized water (15 ml), and Hydrochloric acid (15 ml). The autoclave was then heated to 150°C at different time periods 5, 10, 15, 20, and 25 hours. After allowing the autoclave to cool naturally. The rutile TiO_2 NRs films were deposited on FTO substrate and subsequently washed twice with water is consistent with previous research [19]. The procedure to preparing the MoS_2/TiO_2 composite thin film is described as follows : Thioacetamide (C_2H_5NS) 0.12 g and Sodium molybdate ($Na_2MoO_4.2H_2O$) 0.06 g were dissolved in 40 mL of DI water and stirred magnetically for 40 minutes until a transparent solution was formed . The resulting mixture was then transferred into a 75 mL Teflon-lined stainless steel autoclave containing vertically placed TiO_2 NRs. The autoclave was heated at 200°C for 24 hours to obtain the MoS_2/TiO_2 composite thin film. Finally, the product was washed with DI water and dried at 80°C for 10 hours**.**

The Grätzel model was used to assemble the solar cells, which utilized the MoS_2 /TiO_2/FTO prepared earlier as the photoanode, and an Ag-modified FTO glass as the counter electrode. The solution of electrolyte (Iodoite Z – 100) prepared by combining (0.1 M) LiI, (0.05 M) I_2, and (0.5 M) 4-tert-butylpyridine in acetonitrile. The surface morphology for samples was show by Scanning Electron Microscopy SEM (Supra 55 VP), but the crystal structure of samples was evaluated through XRD technique (land X ' Pert Pro MPD- Philips Nether). The Raman

spectra were recorded using Raman microscopy (Renishaw Invia). The UV-Vis spectrophotometer (Shimadzu UV2100) was used to measure the absorption spectra of the samples. The Current density – Voltage (J -V) curve were measured using a Keithley digital source at 25°C, that simulated sunlight under AM 1.5 G was illumination using Xe- lamp. The active area of solar cells was controlled to be (0.8 cm^2).

3- Results and discussions:

Fig. (1) displays the typical Scanning Electron Microscope (SEM) images of the top - view of TiO_2 NRs films synthesized via hydrothermal method. It can be noticed that densely aligned TiO_2 NRs is covered with uniform on the FTO surface. The shape of the nanorods structure is tetragonal and the top surfaces of all nanorods are square or rectangle [20]. The rate diameter of the nanorods can be seen increased with longer the deposition periods as shown in Table (1). Experiments have shown that TiO_2 NRs do not grow when growth time is less than 3 hours and at 150°C. But when the growth time extends to 30 hours, the TiO_2 NRs membrane begins to peel off from the FTO surface because of the competition between crystal growth and decomposition of the crystals themselves. Fig. (2a) shows the (SEM) images of MoS_2 nanoflowers grown on FTO substrate via hydrothermal method. The high- magnification SEM images revel that MoS_2 randomly grow on FTO substrate with self-assembly nanoflowers ornamented on the surface. The mean length (250 - 260) nm and thickness (18-20) nm of the nanoflowers were determined [21]. Fig. (2b) shows numerous small MoS_2 were present on both the top and side surfaces of TiO_2 nanorods [22].

Table (1): values of rate diameter of the nanorods.

Sample	Period of deposition h	Temp. of deposition °C	Rate diameter of rod nm
T_5	5	150 °C	37.3
T_{10}	10		112.8
T_{15}	15		123.6
T_{20}	20		148.7
T_{25}	25		188.9

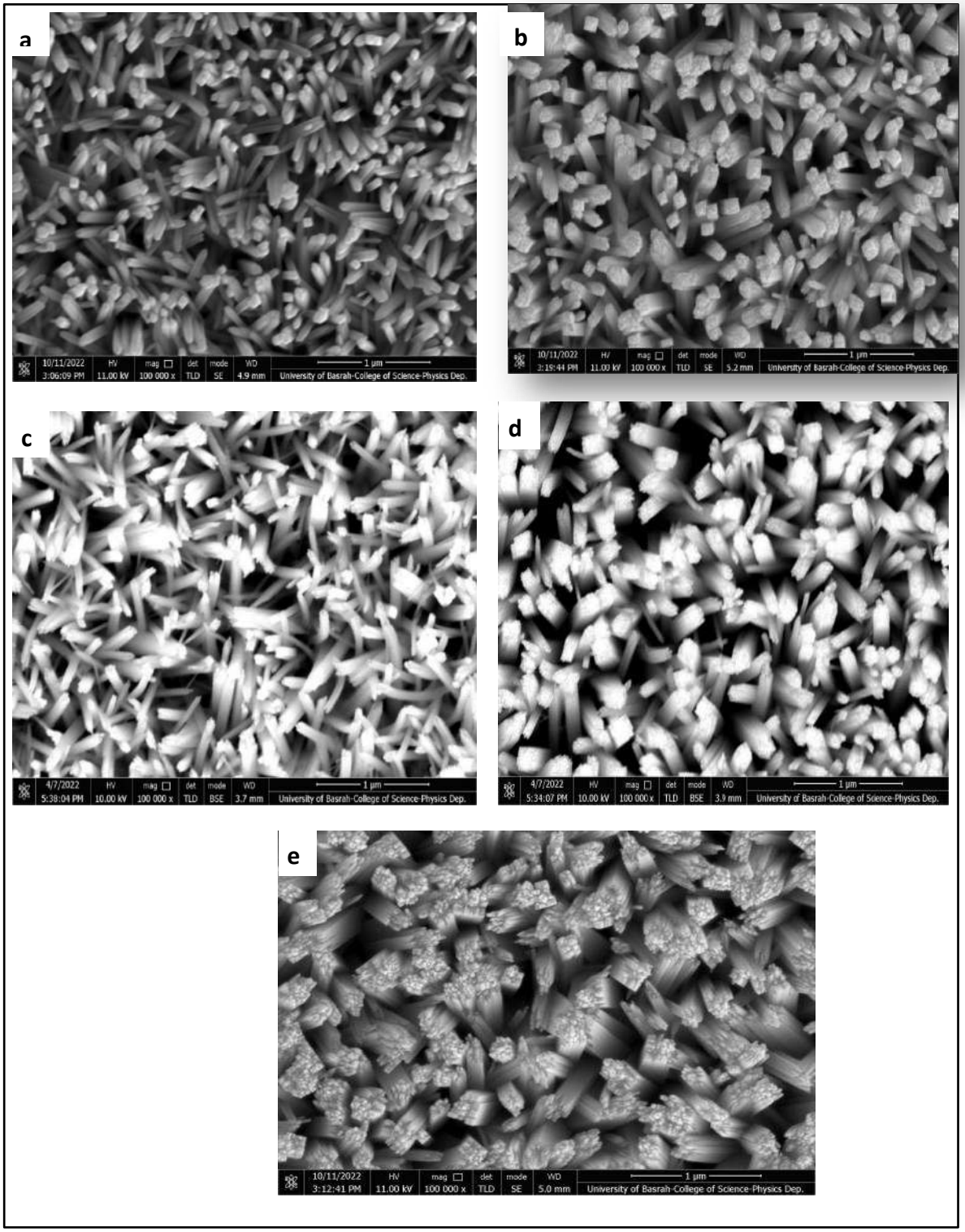

Fig. (1): SEM images of TiO_2 synthesized at 150°C with different reaction times (a) 5 hour, (b) 10 hour, (c) 15 hour, (d) 20 hour, (e) 25 hour.

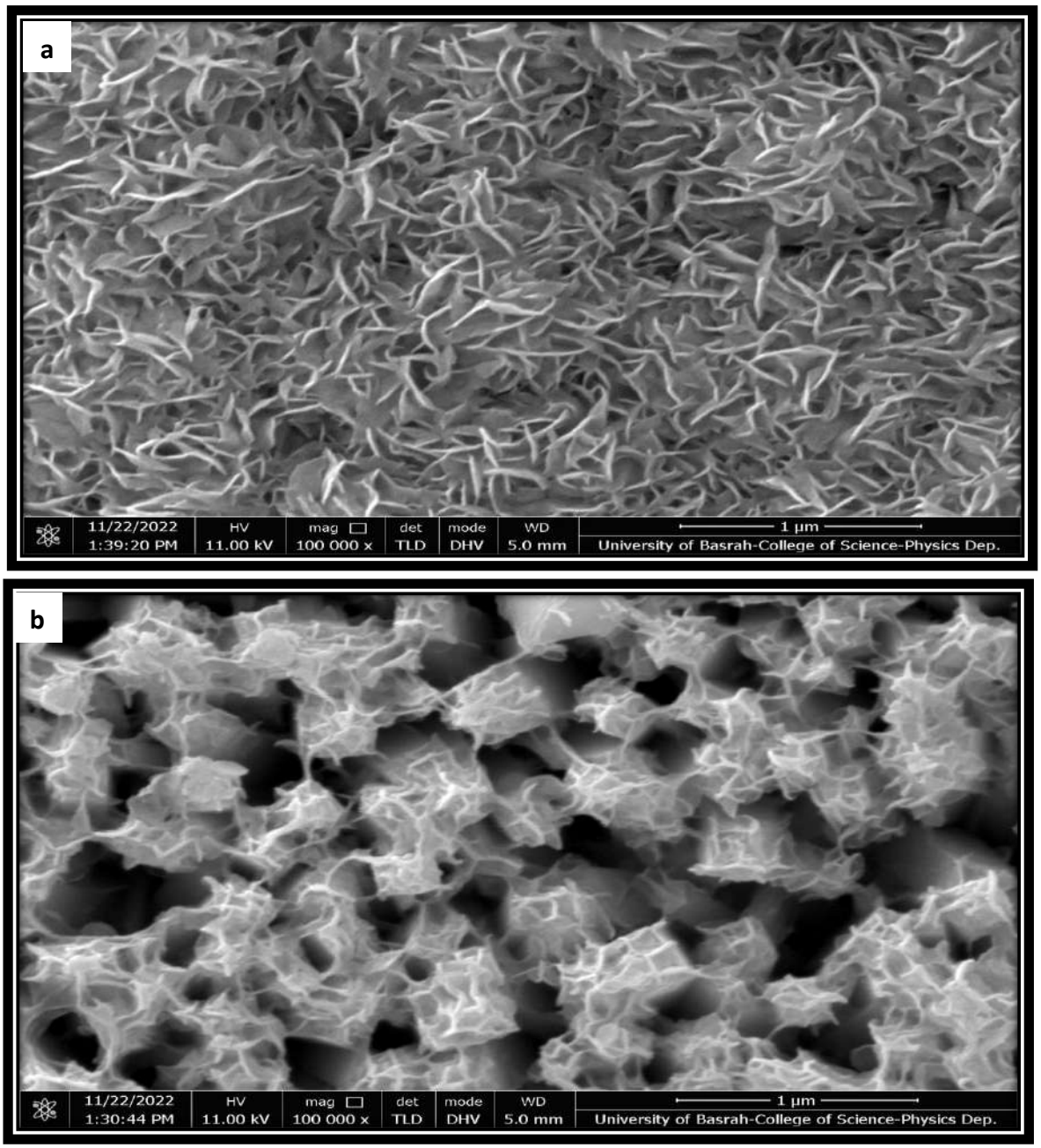

Fig. (2): SEM images of (a) MoS_2 nanoflowers (b) MoS_2/TiO_2.

The X-ray diffraction (XRD) patterns of TiO_2 nanorods array fabricated on an FTO substrate using the hydrothermal method are shown in Figure (3a). The patterns reveal that the films fabricated are matching well with the tetragonal rutile TiO_2 peaks (JCPDS no. 21-1276). The minor lattice mismatch between the rutile phase of TiO_2 and FTO substrate that is the reason for the rutile TiO_2 nanorods are generated instead of other phases such as anatase and brookite. The lattice parameters of both the rutile phase and FTO are very similar with a=b=0.4594 nm and c=0.2958 nm for TiO_2, and a=b=0.4737 nm and c = 0.3185 nm for FTO.

The thin films synthesized with different growth period observed four rutile peaks (110), (101), (002) and (112) at (2θ = 26.86°, 36.08°, 62.74° and 65.92°), respectively. The intensity of the (101) and

(002) peaks increases significantly with an increase in reaction time from 5 to 20 hour, where the growth density of the nanorods is high enough to cover the entire surface of the FTO substrate [21]. However, when the reaction time is extended to 25, the diameter and length of the nanorods are growing at angle on the FTO surface and increased them led to collide with each other. This collision leads to the breakage of some of the rods and the filling of the space between them. As a result, the intensity of the (101) and (002) peaks decreases. High intensity of the (101) peak indicated that TiO_2 NRs have a good crystallization and highly oriented against the FTO substrate in the (001) direction. These results supported by other workers[22]. Fig. (3b) displays the XRD pattern of MoS_2 nanoflowers grown through the hydrothermal method on an FTO substrate. The pattern exhibits prominent diffraction peaks originating from the FTO substrate. Furthermore, weak peaks located at $2\theta = 14.52°$ and $33.88°$ can be observed, which correspond the (002) and (101) planes, respectively, to the standard 2H-MoS_2 (PDF card NO. 37-1492). The strong intensity of the (002) diffraction peak in the sample XRD pattern suggests the formation of a stacked layered structure of MoS_2 [23].

Fig. (4) shows XRD pattern when MoS_2 is deposited on TiO_2 NRs film prepared at a reaction time of 20 hours (M/T_{20}) and it is noted that the characteristic peaks appear for each of the two compounds. In this figure, it is noted that the intensity of the diffraction peaks due to TiO_2 is higher and this is due to recrystallization in the second stage from hydrothermal treatment [24].

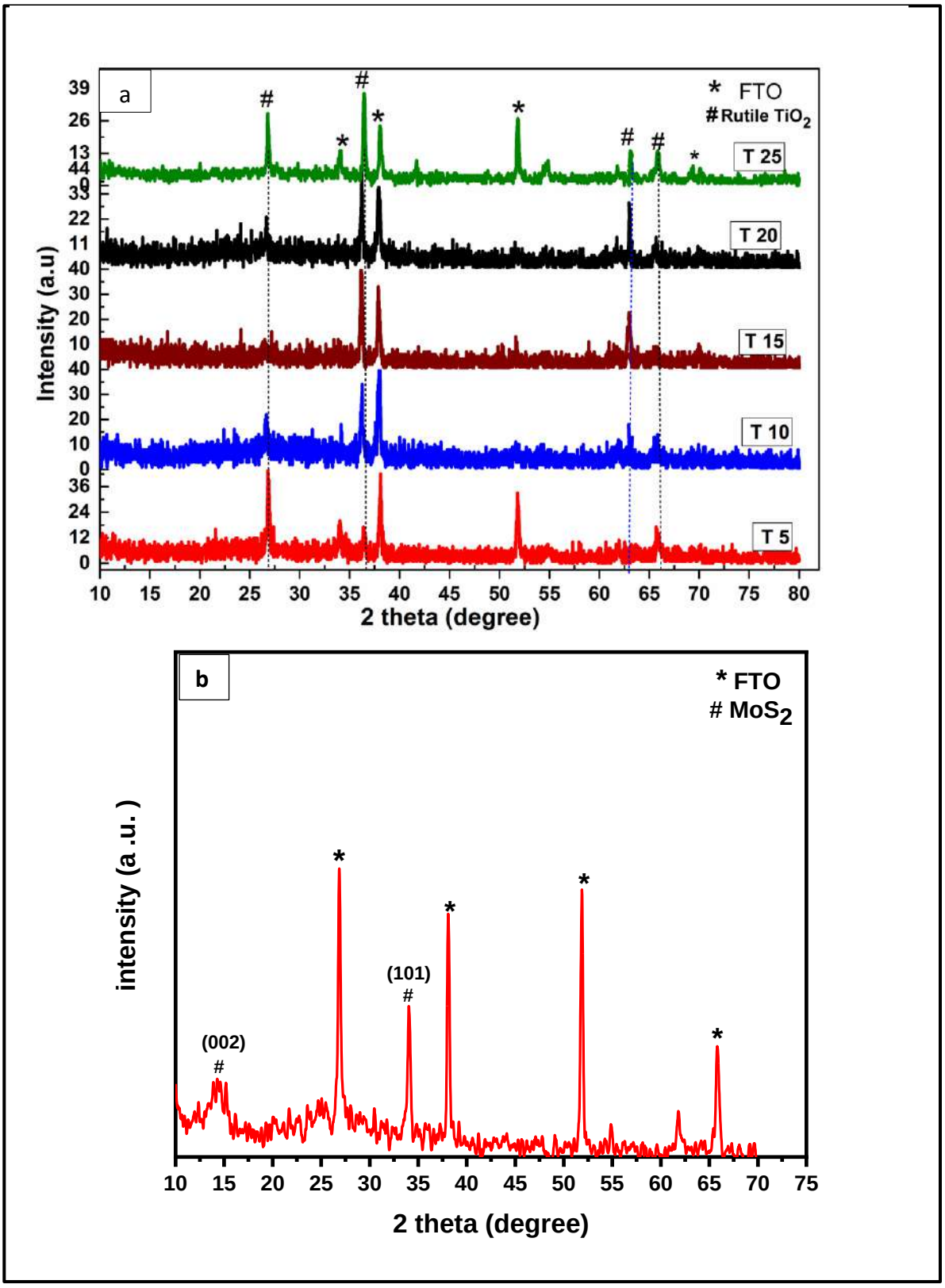

Fig. (3): XRD patterns of (a) TiO_2 at 150°C for different reaction times (b) MoS_2 at 200°C.

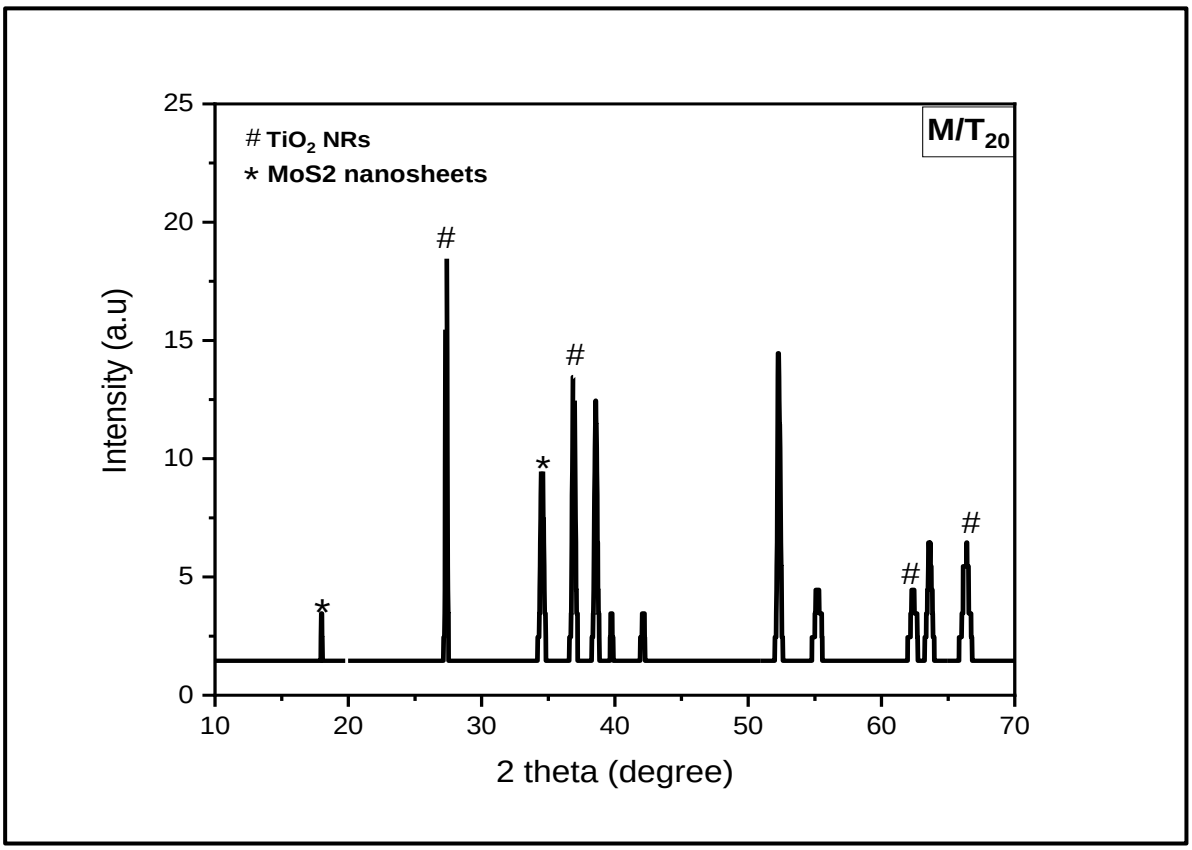

Fig. (4): XRD patterns of MoS_2/TiO_2 (M/T_{20}).

Fig. (5a) shows the Raman spectra of TiO_2 NRs and MoS_2 nanoflowers that was grown on FTO. The Raman curve of TiO_2 NRs displays two resonance peaks centered at 458 and 625 cm^{-1} which correspond to the E_g and A_{1g} vibrational modes of TiO_2 rutile phase, respectively [25]. Fig. (5b) can be well ascribed to the MoS_2 grown on FTO substrate. The Raman scattering peak located at 407 cm^{-1} can be which may be ascribed to E^1_{2g} modes of 2H-MoS_2 [26].

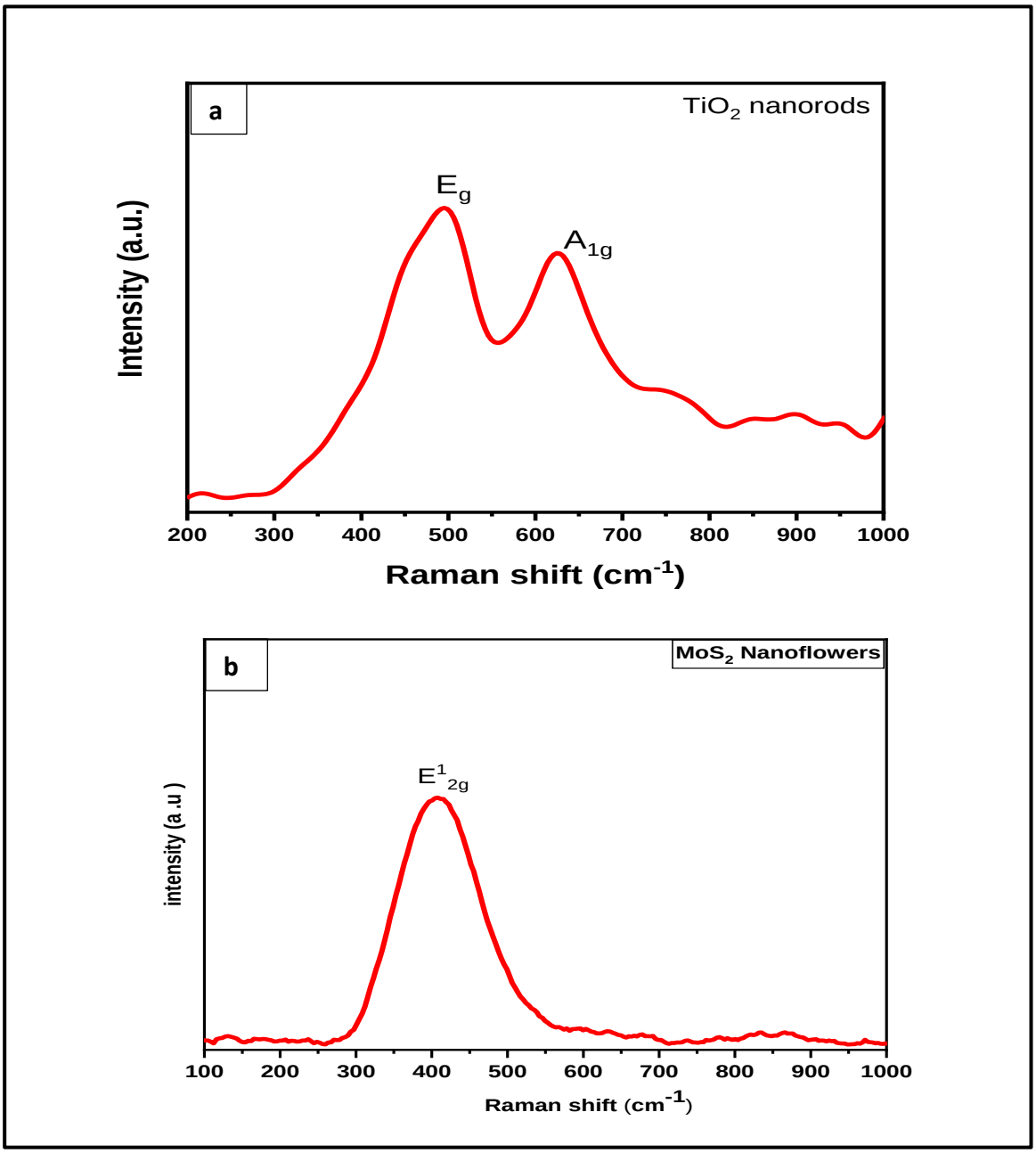

Fig. (5): Raman spectra of (a) TiO_2 nanorods (b) MoS_2 nanoflowers.

Fig. (6) displays the UV-Visible absorption spectra of TiO_2 NRs and MoS_2. The Fig. (6a) represents the absorbance as function to the wavelength for the TiO_2 NRs, that it has evident a sharp absorption edge at around 400 nm and significant absorption in (UV) region when the period of time increase [27]. Fig. (6b) shows the absorption spectrum of MoS_2 where the absorption spectrum within the visible region (400-750) nm and the edge absorption is approximately at 750 nm. Fig. (6c) shows the absorption spectrum obtained when MoS_2 nanoflowers is deposited on the surface of TiO_2 nanorods prepared with a time of 20 hours (M/T_{20}). The intensity of the absorption spectrum is observed to be in the visible region, which can be attributed to the absorption of visible light by MoS_2 nanoflowers. The fig(6c) shows a reduction in the absorbance intensity, which could be attributed to the excessive

stacking of MoS_2. This stacking may lead to a decrease in the material's specific surface area, ultimately causing a decline in its optical performance.

The optical band gap directly allowed transmission which was calculated using the following equation:

$$\alpha h\nu = const\ (h\nu - Eg)^{1/2} \quad -------(1)$$

Where α represent the absorption coefficient, $h\nu$ represent photon energy, and E_g is the band gap.

Fig. (7) depicts a plot of $(\alpha h\nu)^2$ versus energy ($h\nu$), which was utilized to determine the optical band gap. The energy gap was observed to be 3.1, 3.06, 3.02, 2.99, and 2.93 eV for reaction times of 5, 10, 15, 20, and 25 hours, respectively [28]. The decrease in the energy gap value with increasing reaction time can be attributed to the variation in rod length and diameter. As the reaction time increases, the resulting rods are longer and wider suggesting reduced quantum confinement at longer reaction times. The Fig. (7M) displays the direct energy gap of MoS_2 which is approximately 1.7 eV. The results showed that compared to the energy gap of the T_{20} sample, which is around 2.99eV. It will decrease when a MoS_2 is deposited on TiO_2 and the energy gap of the (M/T20) becomes 2.78 eV as shown in the Fig. 8 [12].

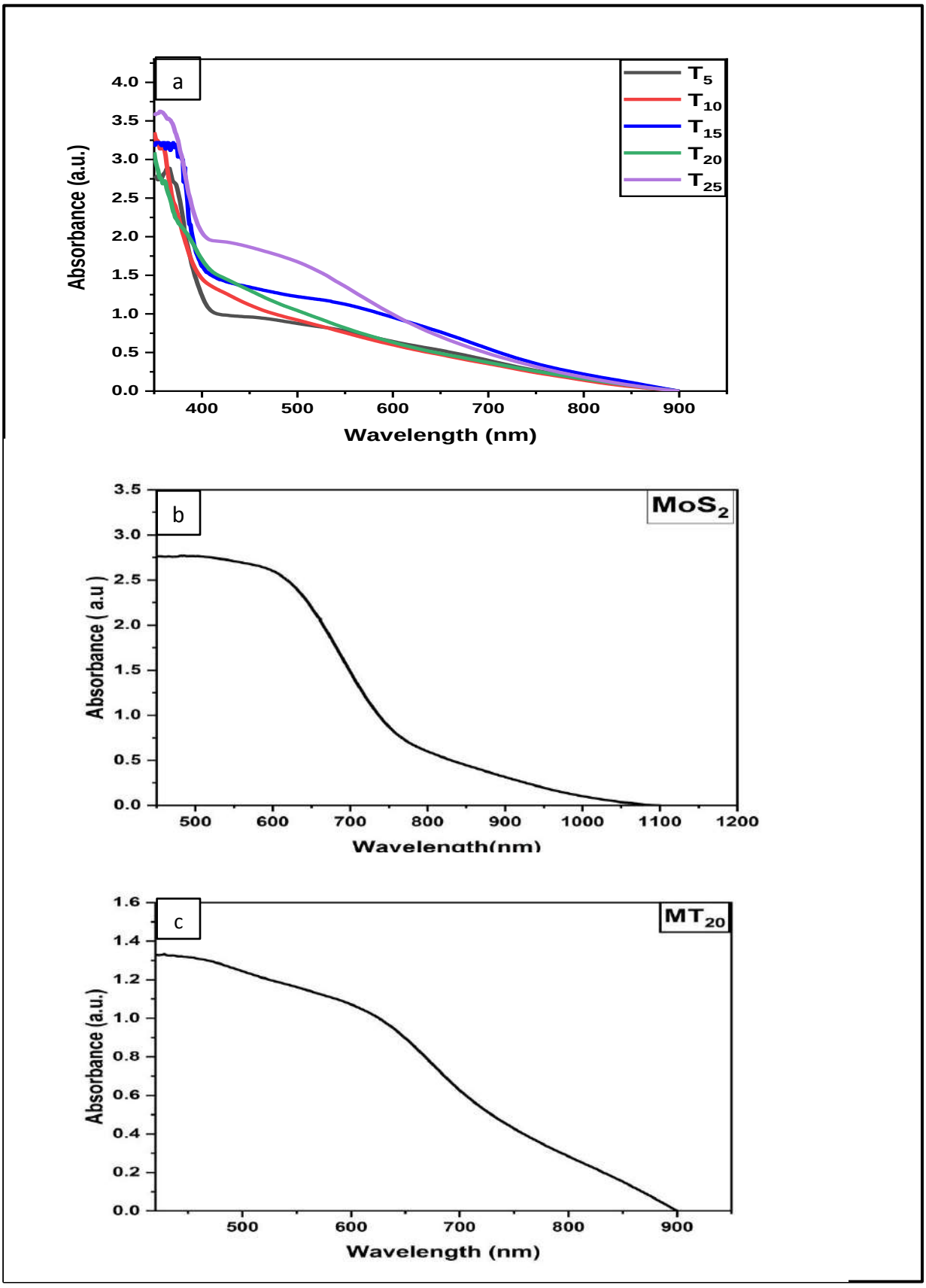

Fig. (6): UV-vis absorbance spectra of the samples (a) TiO_2 NRs (b) MoS_2 (c) M/T_{20}.

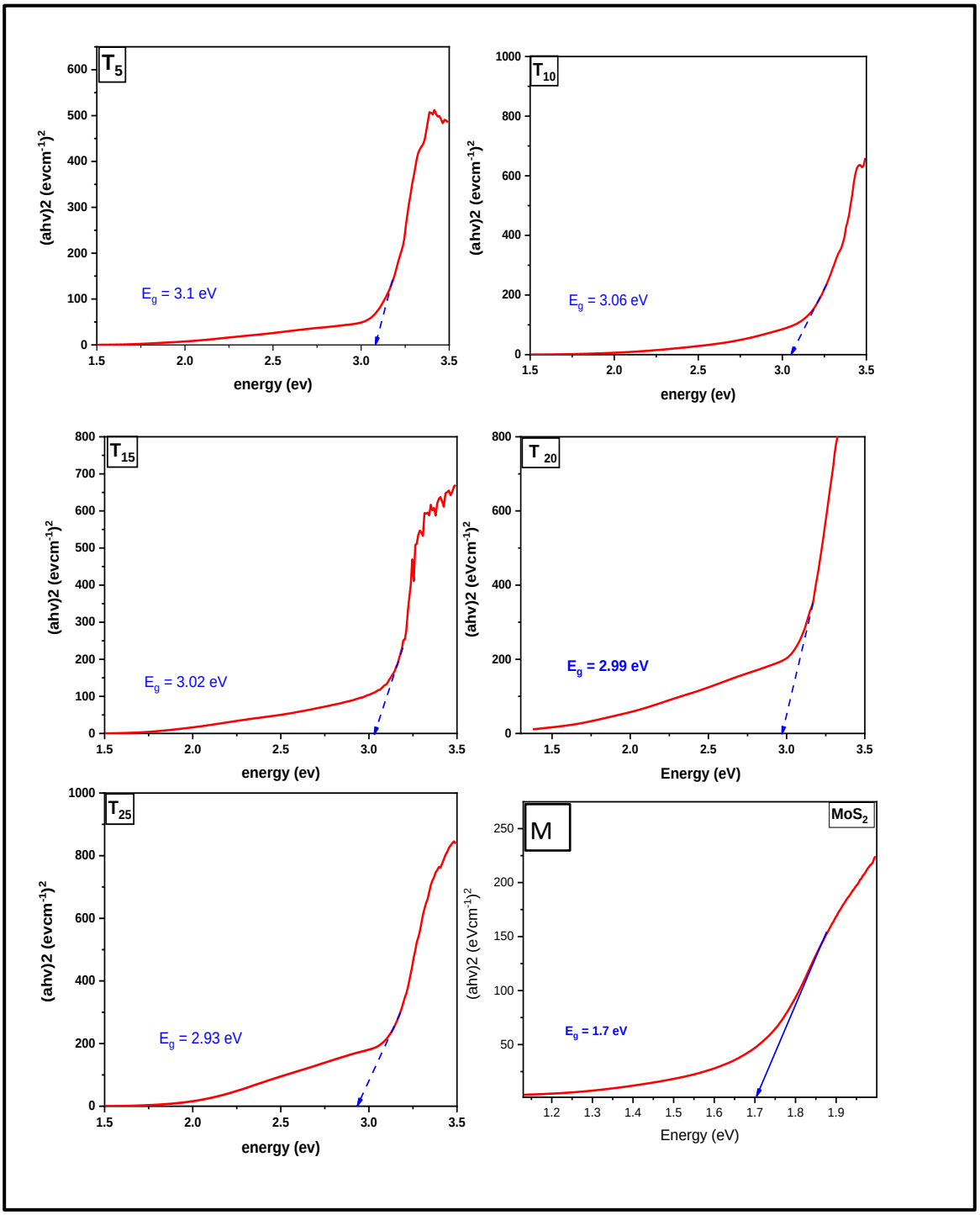

Fig. (7): $(\alpha h\nu)^2$ as a function of ($h\nu$) of TiO_2 NRs (T5) 5 hour (T10) 10 hour (T15) 15 hour (T20) 20 hour (T25) 25 hour (M) MoS_2.

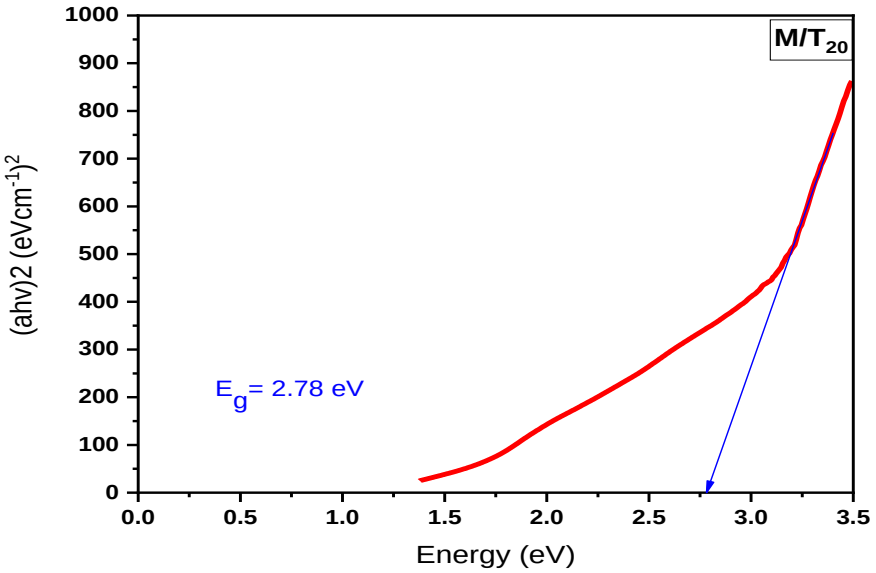

Fig. (8): $(\alpha h\nu)^2$ as a function of ($h\nu$) of M/T20.

The energy level diagram of MoS_2/TiO_2 heterostructure solar cells is illustrated in Figure (9). For effective sensitization, the photo-generated electrons in MoS_2 must migrate to the MoS_2/TiO_2 interface and inject into the conduction band of TiO_2 where they can be extracted to the FTO. Meanwhile, the remaining holes in the valence band of MoS_2 are anticipated to be transported to the electrolyte or any other hole-conductive material. However, significant recombination of electrons and holes transpires at the interface of MoS_2/TiO_2 structure, owing to the presence of a large number of defects in that region. This constitutes the primary reason for the limited efficiency of inorganic semiconductor-sensitized solar cells [29].

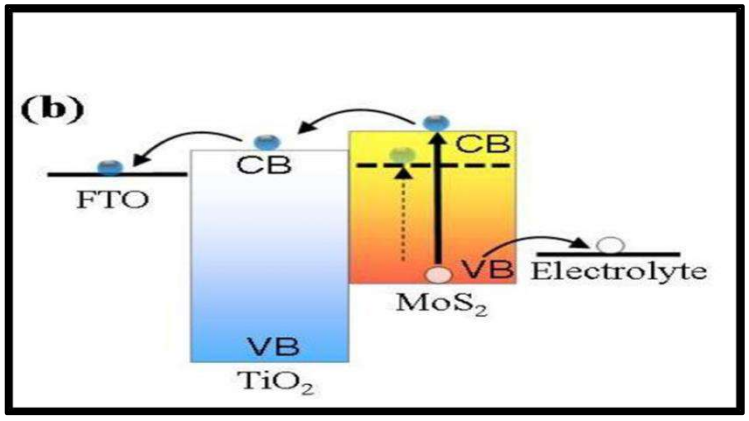

Fig.(9) : Diagram of energy levels of MoS_2/TiO_2.

The Current density - Voltage (J-V) curves of the solar cells based on MoS_2/TiO_2 with varying growth times are depicted in Fig. 10 and Table (2) lists the important parameters of the solar cell, such as the short-circuit current density (J_{SC}), open circuit voltage(V_{OC}), fill factor (FF), and

efficiency(η). The efficiency initially rises to (η = 0.94%) at the time of preparation of the nanorods reaches 20h but decreases again to (η = 0.82%) when time of preparation of TiO_2 reaches 25hour. As the height of the nanorods increases the growth time from (5-20) hour, a greater amount of MoS_2 can adhere to the surface due to the increased surface area leading to improved light absorption and short circuit current density [29]. However, longer growth times 25hour lead to longer nanorods lengths and diameter widths ,as shown in fig(1) resulting in a lower effective internal surface area available for MoS_2 adsorption and therefore a reduction in conversion efficiency [30].

Table (2): Cell parameters of solar cells based on MoS_2/TiO_2.

Sample	J_{SC}	V_{OC}	P_{MAX}	FF	η	R_S	R_{SH}
	mA/cm^2	V	mW/cm^2	%	%	Ω	Ω
M/T_5	2.42	0.328	0.323	40	0.43	508.67	1069.43
M/T_{10}	2.56	0.433	0.421	38	0.56	1260.7	173.33
M/T_{15}	3.22	0.397	0.585	45	0.78	4532.24	122.08
M/T_{20}	4.76	0.379	0.706	39	0.94	1773.09	139.99
M/T_{25}	4.89	0.329	0.613	38	0.82	178.40	34.18

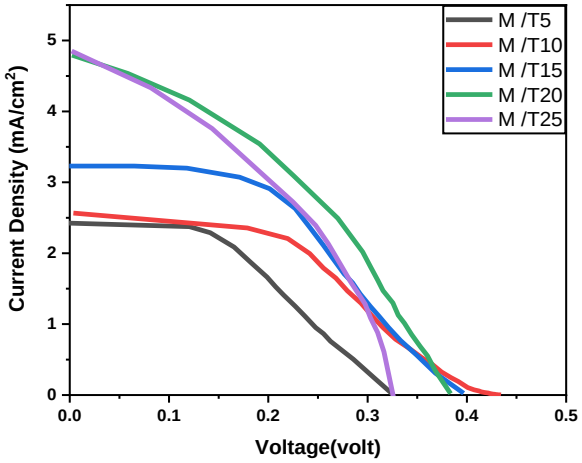

Fig. (10): (J-V) curves of solar cells based MoS_2/TiO_2.

4- Conclusions:

In brief, this study presents approach of integrating low-cost and environmentally friendly semiconductors into 1D nanostructure array to create high performance photovoltaic devices. A

simple hydrothermal method was used to successfully grow of MoS_2/TiO_2 heterostructure and Rutile TiO_2 nanorods were prepared on FTO substrate using various growth durations (5, 10, 15, 20, and 25 hours). The morphology, structure, optical, and electrical properties of the TiO_2 nanorods were observed to be influenced by the duration of growth. The MoS_2 nanosheets has a suitable band gap, which acts as an effective inorganic dye that aids in light absorption and electron transfer in the TiO_2 photoanode. Consequently, the MoS2/TiO_2-based solar cells exhibit a significantly improved power conversion efficiency (PCE) to 0.94%. The improved photo conversion efficiency was linked to the vertically aligned nanorods which were densely arranged and created efficient pathways for the charge carriers generated by light.

REFERENCES

[1] J. Dong *et al.*, "Boosting heterojunction interaction in electrochemical construction of MoS2 quantum dots@ TiO2 nanotube arrays for highly effective photoelectrochemical performance and electrocatalytic hydrogen evolution," *Electrochem. commun.*, vol. 93, pp. 152–157, 2018.

[2] M. D. Patel, J. Zhang, J. Park, N. Choudhary, J. M. Tour, and W. Choi, "Directly deposited porous two-dimensional MoS2 films as electrocatalysts for hydrogen evolution reactions," *Mater. Lett.*, vol. 225, pp. 65–68, 2018.

[3] "Influence of growth time on structural, optical and electrical properties of TiO2 nanorod arrays deposited by hydrothermal method," *Surf. Rev. Lett.*, vol. 26, no. 03, p. 1850155, 2019.

[4] J. Wan *et al.*, "Hydrothermal etching treatment to rutile TiO 2 nanorod arrays for improving the efficiency of CdS-sensitized TiO 2 solar cells," *Nanoscale Res. Lett.*, vol. 11, pp. 1–9, 2016.

[5] X. Feng, K. Zhu, A. J. Frank, C. A. Grimes, and T. E. Mallouk, "Rapid charge transport in dye-sensitized solar cells made from vertically aligned single-crystal rutile TiO2 nanowires," *Angew. Chemie*, vol. 124, no. 11, pp. 2781–2784, 2012.

[6] R. R. Chianelli *et al.*, "Catalytic properties of single layers of transition metal sulfide catalytic materials," *Catal. Rev.*, vol. 48, no. 1, pp. 1–41, 2006.

[7] S. Dey and S. C. Roy, "Designing TiO2 nanostructures through hydrothermal growth: influence of process parameters and substrate position," *Nano Express*, vol. 2, no. 1, p. 10028, 2021.

[8] M. Lv *et al.*, "Optimized porous rutile TiO 2 nanorod arrays for enhancing the efficiency of dye-sensitized solar cells," *Energy Environ. Sci.*, vol. 6, no. 5, pp. 1615–1622, 2013.

[9] C. J. Howard, T. M. Sabine, and F. Dickson, "Structural and thermal parameters for rutile and anatase," *Acta Crystallogr. Sect. B Struct. Sci.*, vol. 47, no. 4, pp. 462–468, 1991.

[10] Y. Li, M. Zhang, M. Guo, and X. Wang, "Hydrothermal growth of well-aligned TiO 2 nanorod arrays: Dependence of morphology upon hydrothermal reaction conditions," *Rare Met.*, vol. 29, pp. 286–291, 2010.

[11] M. Ye, H. Liu, C. Lin, and Z. Lin, "Hierarchical Rutile TiO2 Flower Cluster-Based High Efficiency Dye-Sensitized Solar Cells via Direct Hydrothermal Growth on Conducting Substrates," *Small*, vol. 9, no. 2, pp. 312–321, 2013.

[12] J. Xu *et al.*, "Growth of MoS2 nanoflakes and the photoelectric response properties of MoS2/TiO2 NRs compositions," *J. Mater. Sci. Mater. Electron.*, vol. 30, no. 24, pp. 21465–21476, 2019.
[13] R. I. Christy, "Sputtered MoS2 lubricant coating improvements," *Thin Solid Films*, vol. 73, no. 2, pp. 299–307, 1980.
[14] Q. H. Wang, K. Kalantar-Zadeh, A. Kis, J. N. Coleman, and M. S. Strano, "Electronics and optoelectronics of two-dimensional transition metal dichalcogenides," *Nat. Nanotechnol.*, vol. 7, no. 11, pp. 699–712, 2012.
[15] Q. Xiong *et al.*, "One-step synthesis of cobalt-doped MoS 2 nanosheets as bifunctional electrocatalysts for overall water splitting under both acidic and alkaline conditions," *Chem. Commun.*, vol. 54, no. 31, pp. 3859–3862, 2018.
[16] J. N. Coleman *et al.*, "Two-dimensional nanosheets produced by liquid exfoliation of layered materials," *Science (80-.).*, vol. 331, no. 6017, pp. 568–571, 2011.
[17] X. Ren *et al.*, "2D co-catalytic MoS2 nanosheets embedded with 1D TiO2 nanoparticles for enhancing photocatalytic activity," *J. Phys. D. Appl. Phys.*, vol. 49, no. 31, p. 315304, 2016.
[18] Z. H. Nasser, S. J. Kasim, and W. S. Hanoosh, "Growth, Single-Crystalline Rutile TiO2 Nanorod Thin Film By Hydrothermal Technique," *J. Kufa-Physics*, vol. 10, no. 2, 2018.
[19] J. Xi, O. Wiranwetchayan, Q. Zhang, Z. Liang, Y. Sun, and G. Cao, "Growth of single-crystalline rutile TiO 2 nanorods on fluorine-doped tin oxide glass for organic–inorganic hybrid solar cells," *J. Mater. Sci. Mater. Electron.*, vol. 23, pp. 1657–1663, 2012.
[20] H. Miao *et al.*, "Hydrothermal synthesis of MoS2 nanosheets films: Microstructure and formation mechanism research," *Mater. Lett.*, vol. 166, pp. 121–124, 2016.
[21] A. Prathan *et al.*, "Controlled structure and growth mechanism behind hydrothermal growth of TiO2 nanorods," *Sci. Rep.*, vol. 10, no. 1, pp. 1–11, 2020.
[22] F. Guo *et al.*, "Controlled growth of highly pure TiO 2 nanorod arrays/nanoflower clusters via one-step hydrothermal route," *J. Mater. Sci. Mater. Electron.*, vol. 29, pp. 12169–12177, 2018.
[23] H. N. T. Phung, V. N. K. Tran, L. T. Nguyen, L. K. T. Phan, P. A. Duong, and H. V. T. Le, "Investigating visible-photocatalytic activity of MoS2/TiO2 heterostructure thin films at various MoS2 deposition times," *J. Nanomater.*, vol. 2017, 2017.
[24] D. Qi, S. Li, Y. Chen, and J. Huang, "A hierarchical carbon@ TiO2@ MoS2 nanofibrous composite derived from cellulose substance as an anodic material for lithium-ion batteries," *J. Alloys Compd.*, vol. 728, pp. 506–517, 2017.
[25] M. Shen, Z. Yan, L. Yang, P. Du, J. Zhang, and B. Xiang, "MoS 2 nanosheet/TiO 2 nanowire hybrid nanostructures for enhanced visible-light photocatalytic activities," *Chem. Commun.*, vol. 50, no. 97, pp. 15447–15449, 2014.
[26] X. Li and H. Zhu, "Two-dimensional MoS2: Properties, preparation, and applications," *J. Mater.*, vol. 1, no. 1, pp. 33–44, 2015.
[27] M. H. Nguyen and K.-S. Kim, "Analysis on growth mechanism of TiO2 nanorod structures on FTO glass in hydrothermal process," *J. Ind. Eng. Chem.*, vol. 104, pp. 445–457, 2021.
[28] Y. Gao *et al.*, "TiO2 nanorod arrays based self-powered UV photodetector: heterojunction

with NiO nanoflakes and enhanced UV photoresponse," *ACS Appl. Mater. Interfaces*, vol. 10, no. 13, pp. 11269–11279, 2018.

[29] T. Du, N. Wang, H. Chen, H. He, H. Lin, and K. Liu, "TiO2-based solar cells sensitized by chemical-bath-deposited few-layer MoS2," *J. Power Sources*, vol. 275, pp. 943–949, 2015, doi: 10.1016/j.jpowsour.2014.11.048.

[30] X. Gan *et al.*, "Controlling the spontaneous emission rate of monolayer MoS2 in a photonic crystal nanocavity," *Appl. Phys. Lett.*, vol. 103, no. 18, p. 181119, 2013.